PROCEEDINGS OF SCIENCE

Medium-energy (few TeV - 100 TeV) neutrino point source searches in the Southern sky with IceCube

The IceCube Collaboration[†],

[†] *http://icecube.wisc.edu/collaboration/authors/icrc15_icecube*

E-mail: david.altmann@desy.de

Many galactic sources of gamma rays are suspected to also produce high-energy neutrinos with a typical high-energy cutoff below 100 TeV. At the location of IceCube, the Galactic Center and a large fraction of the Galactic Plane lie continuously above the horizon, where the large background of atmospheric muons makes any search for galactic neutrino sources extremely challenging. This background can be significantly reduced by using the outer portion of the detector as a veto and by applying event topology cuts. The data were taken during the first year of the completed IceCube detector and correspond to a livetime of 337 days. The event selection, optimized for neutrino energies between a few TeV and 100 TeV, is presented along with the results for a southern sky point source scan and the investigation of selected sources.

Corresponding authors: D. Altmann[1,2*], A. Kappes[2],

[1] *DESY, Platanenallee 8, 15378 Zeuthen, Germany*

[2] *ECAP, Physikalisches Institut, Erwin-Rommel-Straße 1, 91058 Erlangen, Germany*

The 34th International Cosmic Ray Conference,
30 July- 6 August, 2015
The Hague, The Netherlands

*Speaker.

PoS(ICRC2015)1056

1. Introduction

The southern sky provides a large variety of interesting objects for a search of point-like sources of astrophysical neutrinos, such as the galactic center and numerous other potential neutrino sources [1, 2, 3, 4]. Gamma-ray spectra observed by FERMI or HESS suggest some of these objects produce gamma rays by hadronic mechanisms[5]. However, for most of them the separation between hadronic or leptonic production is not obvious. The detection of neutrinos from these sources with IceCube would provide us with a better understanding of the source environment.

IceCube is a cubic-kilometer neutrino detector installed in the ice at the geographic South Pole [6] between depths of 1450 m and 2450 m. Detector construction started in 2005 and finished in 2010. Neutrino reconstruction relies on the optical detection of Cerenkov radiation emitted by secondary particles produced in neutrino interactions in the surrounding ice or the nearby bedrock.

Traditionally, the ν_μ charged-current channel is the preferred signal, since the muons produced leave a track-like pattern in the detector. This pattern can be reconstructed with good angular precision (for most energies better than two degrees). Thus, the reconstructed direction of the muon points back to the source of the neutrino. However, in the southern sky this scheme is challenging due to the large background of muons produced in the atmosphere. In recent years, several IceCube searches [7, 8, 9] which select neutrino events interacting inside the detector volume (so called "starting" events), proved to be very successful – most known for the detection of the high-energy astrophysical neutrino flux [8].

This contribution presents a new selection of data taken during the first year of operation of the completed IceCube detector. The selection discussed in this paper is optimized for the detection of "starting" events from interactions of ν_μ with energies between a few TeV and 100 TeV (called in what follows STeVE, Starting TeV Events). An analysis concentrating on lower energies (below few TeV), Low-Energy Starting Event (LESE) is discussed in [10], and an analysis focusing on Medium-Energy (100 TeV - 1 PeV) Starting Events (MESE) has been presented in [11].

2. Data selection

The main challenge for the STeVE analysis is the vast background of muons. A very successful way to separate these muons from neutrinos is the selection of starting tracks. A starting track is an event where a neutrino interacts within the detector volume and produces a muon. The hadronic cascade at the interaction vertex and the muon create a hit pattern that does not start at the edges of the detector, but somewhere inside the detector volume. In principle such a pattern can only be produced by a neutrino. However, due to the relatively large string separation of IceCube, 125 m, atmospheric muons can pass through the outer layers of the detector and mimic a hit pattern that is very similar to that of a starting event neutrino interaction.

A first selection step is the implementation of an event filter that is optimized to keep as many starting events as possible while rejecting over 90 percent of the atmospheric muons, reducing the event rate from about 2200 events per second at trigger level to about 190 events per second. For this, the starting vertex of the event is reconstructed if the event passes a pre-selection, based on the position and type of the hit pattern in the detector (see [10] for more detail on the pre-selection

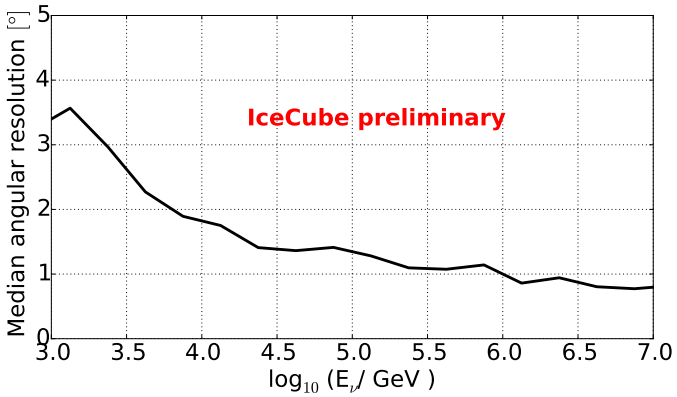

Figure 1: Median angular resolution of simulated muon neutrinos in the event sample plotted as a function of true neutrino energy.

and [12] for details on the reconstruction algorithm). If the vertex is within the contained volume, the event is kept. After this initial step, the data selection of the LESE and STeVE analyses differ.

The usage of advanced reconstruction methods is computationally expensive. Therefore, the event sample is reduced by an energy cut to a rate of about 7 events/s. For this reduced sample, the direction is reconstructed again with a more accurate algorithm using the multiple photoelectron PDF [13] that describes the arrival time of the first of multiple photons. Since the optical properties of the glacial ice at the South Pole are not uniform with depth, we calculate these PDFs with a Monte-Carlo using a realistic ice model [14] and then fit the PDFs with splines [15]. Then the stochastic energy losses along the reconstructed track are calculated using the unfolding algorithm discussed in [16].

The stochastic energy loss pattern provided by the unfolding is then used to calculate several variables based on the energy and length of the event, like the initial energy deposition of the track or the depth inside the detector of the initial energy deposition. With these and other track reconstruction variables, a Boosted Decision Tree (BDT) is trained. The final cut on the BDT score is then optimized to provide the optimal sensitivity for a point-like source search. During data taking operation, the IceCube detector can run with incomplete configurations of strings. Though these runs are rare, they can be problematic for an event selection that uses the event topology as a main selection criterion; therefore, they are excluded, reducing the livetime by about 30 days.

At final level, the event sample consists of 10178 events. Most of these events are expected to be remaining atmospheric muons. The number of background events is reduced by a factor of about 10^7. Roughly 20 percent of all starting muon tracks from neutrino interactions within the detector volume and $E_\nu > 10\,\mathrm{TeV}$ are kept. The median angular resolution is shown in Fig. 1. Compared to other point source searches [17], the resolution is somewhat worse, mainly due to the shorter length of the events compared to a through-going event sample. The effective area of this analysis at final cut level is shown in Fig. 2.

3. Analysis method

To calculate the probability that an excess of events at a certain position is due to a fluctuation

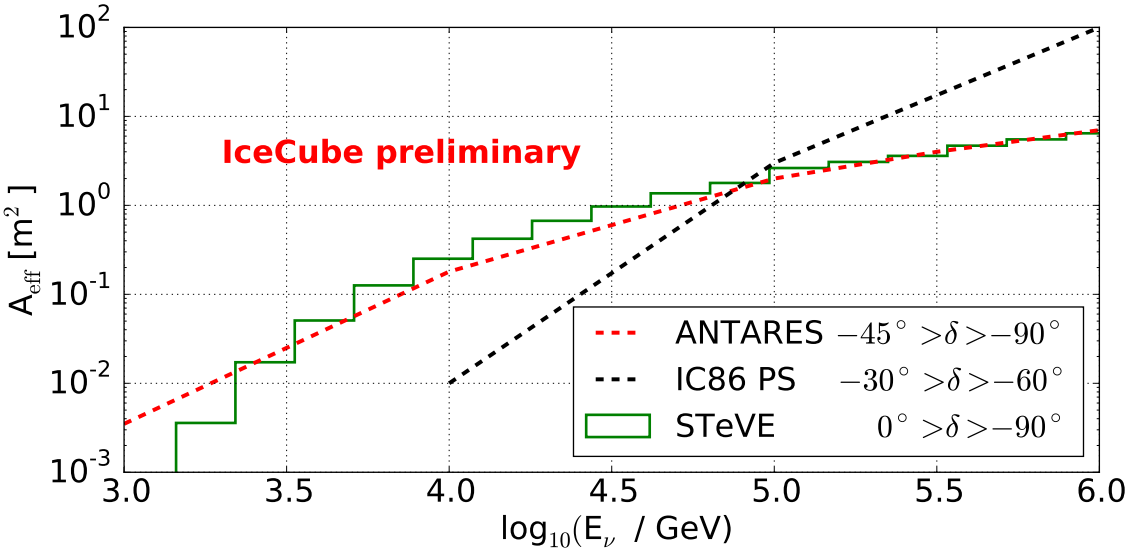

Figure 2: Effective area of the STeVE analysis compared to the IC86 through-going PS analysis (marked as IC86 PS) [17] and ANTARES [18]. δ is the declination of the neutrino event.

of the background, an unbinned maximum likelihood method [19] is used. For a given event and location in the sky, we compute the PDFs S_i and B_i describing the compatibility of the event with the signal and background hypotheses, respectively. These PDFs depend on the event energy and the angular difference between the reconstructed event direction and the location in the sky. The shape of the signal pdf depends on the spectral index γ and, in some investigated scenarios, on the cutoff in energy. The PDF, $f(n_s)$, describing the event under the combined signal and background hypothesis, is given in equation 3.1, where N is the number of events in the sample and n_s is a free parameter to select the relative weight of the signal and background PDFs. For the entire data set, the product of the single event probabilities defines the likelihood ($\mathscr{L}$), shown in eq. 3.2. For a hypothetical point source location, $\mathscr{L}$ is maximized over the data set with respect to n_s and signal spectral index (γ), giving the best-fit values $\hat{n}_s$ and $\hat{\gamma}$. The signal hypothesis is compared to the background hypothesis of no signal ($n_s = 0$). The ratio of both hypotheses yields the test statistic (TS) shown in eq. 3.3.

$$f(n_s) = \frac{n_s}{N} S_i + \left(1 - \frac{n_s}{N}\right) B_i \tag{3.1}$$

$$\mathscr{L}(n_s) = \prod_i^N [f(n_s)] \tag{3.2}$$

$$\mathrm{TS} = -2\log\left(\frac{\mathscr{L}(n_s = 0)}{\mathscr{L}(\hat{n}_s, \hat{\gamma})}\right) \tag{3.3}$$

The distribution of the TS for the null-hypothesis is assessed by generating a few thousand pseudo-experiments, which are created by scrambling the events in right ascension. Then for each of the scrambled skies, the TS at the investigated point is calculated. These TS distributions can differ for different zenith bands. Therefore, the zenith-independent p-value = $\eta \cdot \chi^2(ndof, TS)$ is

Source	$\hat{n}_s$	$\hat{\gamma}$	p-value	$\Phi^{90\%}_{\nu_\mu+\bar{\nu}_\mu} \times 10^{-12}\,\mathrm{TeV}^{-1}\mathrm{cm}^{-2}\mathrm{s}^{-1}$		
				No E_{cut}	E_{cut} = 100 TeV	E_{cut} = 10 TeV
HESS J1458-608	3.96	2.6	79.2 %	203	432	6506
HESS J1837-069	5.18	3.2	85.7 %	175	258	1172
SNR G000.9+00.1	8.14	4.0	35.4 %	295	560	3659
Terzan 5	3.41	2.9	98.9 %	231	414	2952
HESS J1507-622	4.09	2.7	85.9 %	203	423	6813
HESS J1841-055	4.77	3.3	91.3 %	159	236	909

Table 1: Table of all sources with post trial background probability smaller than 100%. Listed are the signalness parameter $\hat{n}_s$, the fitted spectral index $\hat{\gamma}$, the calculated background probability after trial-correction and the upper limit on the flux for an E^{-2} spectrum without a cutoff and two scenarios with a hard cutoff in units of $10^{-12}\,\mathrm{TeV}^{-1}\mathrm{cm}^{-2}\mathrm{s}^{-1}$.

used. Here η is the correction factor for the TS=0 values, caused by the restriction to a positive signal-parameter n_s, and $ndof$ is the number of effective degrees of freedom, computed by a fit of a χ^2 function to the tail of the TS distribution. Based on these TS distributions one can calculate how likely a certain value is. If one does not look at a single point in the sky, but a few (like in a source list) or many (like in an all-sky scan), the trial factor has to be considered. For this, again, we use scrambled skies and then calculate, for the entire investigated ensemble of points, the distribution of maximal -$\log_{10}$(p-value). Based on this distribution the probability to measure a source that is at least as unlikely as the measured one can be calculated.

We used two approaches to search for potential point-like sources:

3.1 Source list

The source list is mainly based on TeVCat sources [20]. Here, all sources in the southern sky (84) are selected. Additionally, 12 source candidates that were under investigation in previous IceCube searches for point-like sources (see [17]) but are not in the TeVCat are added.

Of the 96 investigated sources, none showed a significant over-fluctuation after correcting for trial factors. SNR G000.9+00.1 is the source with the smallest background probability of 0.5% before trial correction. After trial correction this source has a background probability of 35.4%. The six sources with the lowest background probability are shown in Table 1. Upper limits were calculated using the Neyman method [21]. The sensitivity, discovery potential and upper limits for the investigated sources, assuming a scenario with an E^{-2} dependence on neutrino energy with a cutoff of 100 TeV, are shown in Fig. 3.

3.2 Southern sky scan

Additionally, we scanned the southern sky with a HEALPix[1] [23] grid with a bin width of about 0.46 degree. This is well below the angular resolution of the sample (as shown in Fig 1). For each point, the background probability was calculated in the same way as for the source list, resulting in the skymap shown in Fig. 4. The point with the lowest background probability is found at right ascension 93.1°, declination -64.3°. Correcting for the trial factor yields a probability of

[1] http://healpix.sourceforge.net

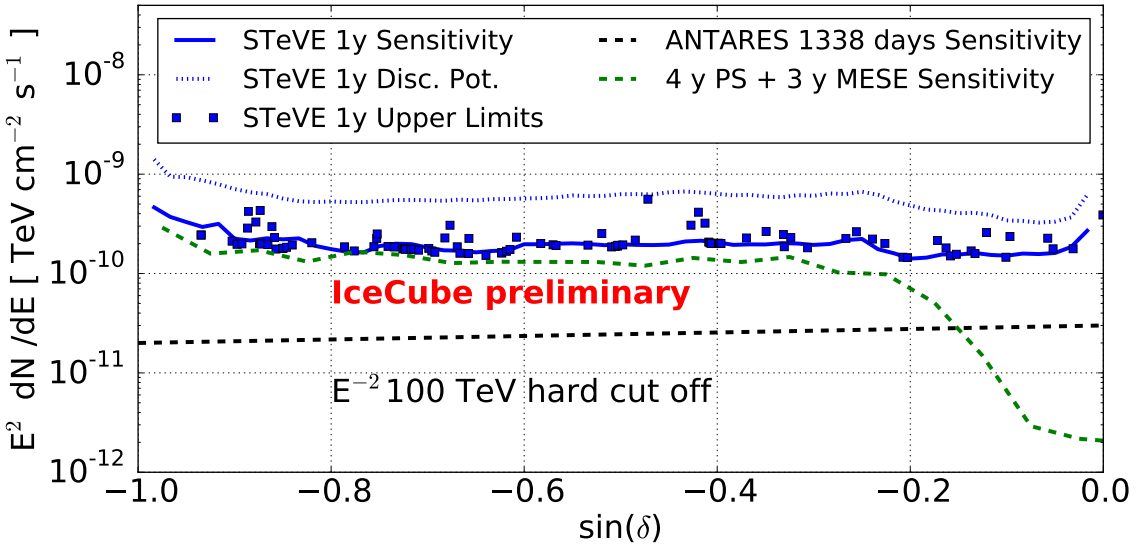

Figure 3: Sensitivities for STeVE (solid line), ANTARES [22] and the combined MESE [11] and through-going IceCube point-like source search [17] (dashed lines) with their respective livetimes. Additionally, the discovery potential (dotted) and upper-limits on the investigated sources for the STeVE analysis (squares) are shown. The assumed spectrum is E^{-2} with a hard cutoff at 100 TeV.

74.9% that a background fluctuation at least as significant happened anywhere in the observed sky during the observation time. Thus, the results of the sky scan are fully compatible with the background-only hypothesis.

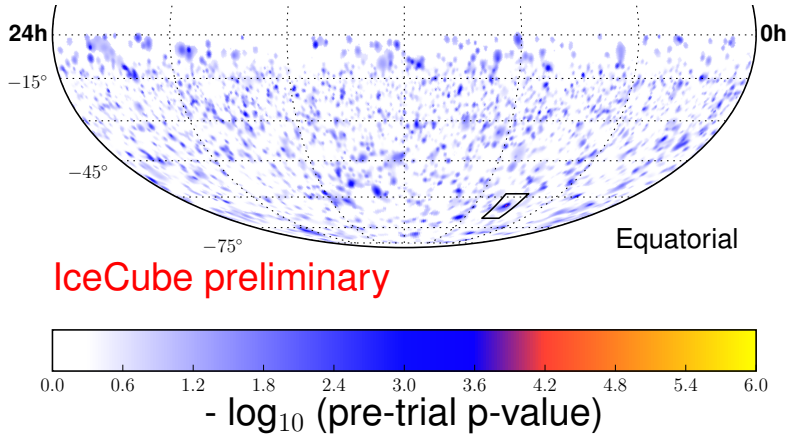

Figure 4: Fitted p-values in the southern sky. The point with the lowest background probability is found at right ascension 93.1°, declination -64.3° (in the center of the black rectangle).

4. Conclusions

The STeVE analysis has not found any indication for a point-like source of neutrino emission in the southern sky using data corresponding to 337 days of detector livetime. For the energy

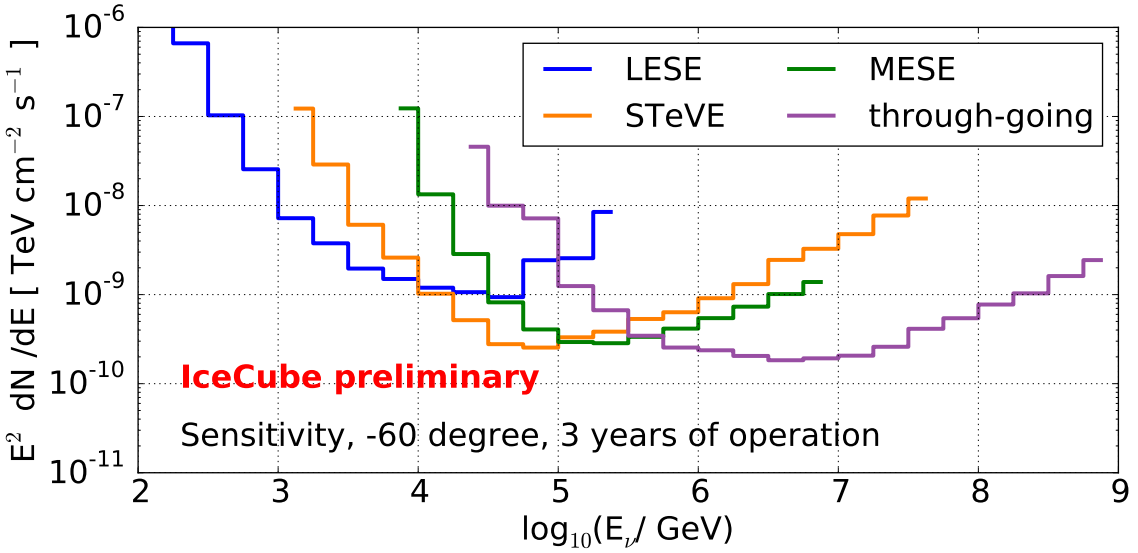

Figure 5: The differential sensitivities for four IceCube point-like source searches in the southern sky. The sensitivities for LESE [10], STeVE and the through-going analysis [17] are estimated simulating events with a livetime of MESE [11].

region of interest below 100 TeV, the 90% C.L. upper limits are competitive with other IceCube results. This could be achieved with a livetime of one year compared to the combined three year MESE / four year through-going IceCube point-like source search. However, due to worse angular resolution and higher number of background events, the presented limits are not yet very competitive with the limits of the searches with ANTARES [22]. A combination of LESE/STeVE/MESE and through-going IceCube point-like source searches would cover an unprecedented energy range from a few 100 GeV to EeV (see Fig. 5).

References

[1] A. Kappes, J. Hinton, C. Stegmann, and F. A. Aharonian, *Astrophys.J.* **656** (2007), no. 2 870.

[2] M. D. Kistler and J. F. Beacom, *Phys.Rev.* **D74** (2006) 063007, [astro-ph/0607082].

[3] F. Vissani and F. Aharonian, *Nucl.Instrum.Meth.* **A692** (Nov., 2012) 5–12, [arXiv:1112.3911].

[4] Q. Yuan, P.-F. Yin, and X.-J. Bi, *Astropart.Phys.* **35** (Aug., 2011) 33–38, [arXiv:1010.1901].

[5] **Fermi-LAT** Collaboration, M. Ackermann et al., *Science* **339** (2013) 807, [arXiv:1302.3307].

[6] **IceCube** Collaboration, A. Achterberg et al., *Astropart.Phys.* **26** (2006), no. 3 155 – 173.

[7] **IceCube** Collaboration, M. Aartsen et al., *Science* **342** (2013) 1242856, [arXiv:1311.5238].

[8] **IceCube** Collaboration, M. Aartsen et al., *Phys.Rev.* **D91** (2015), no. 2 022001, [arXiv:1410.1749].

[9] **IceCube** Collaboration, M. Aartsen et al., *Phys.Rev.Lett.* **113** (2014) 101101, [arXiv:1405.5303].

[10] **IceCube** Collaboration, M. Aartsen et al., *Low-energy (100 GeV - few TeV) neutrino point source searches in the Southern sky with IceCube* , in *PoS(ICRC2015)1053, these proceedings*, 2015.

[11] J. Feintzeig, *Searches for Point-like Sources of Astrophysical Neutrinos with the IceCube Neutrino Observatory*. PhD thesis, University of Wisconsin, Madison, 2014.

[12] S. Euler, *Observation of oscillations of atmospheric neutrinos with the IceCube Neutrino Observatory*. PhD thesis, RWTH Aachen, 2014.

[13] **AMANDA** Collaboration, J. Ahrens et al., *Nucl.Instrum.Meth.* **A524** (2004) 169–194, [astro-ph/0407044].

[14] **IceCube** Collaboration, M. Aartsen et al., *Nucl.Instrum.Meth.* **A711** (2013) 73–89, [arXiv:1301.5361].

[15] N. Whitehorn, J. van Santen, and S. Lafebre, *Comput.Phys.Commun.* **184** (2013) 2214–2220, [arXiv:1301.2184].

[16] **IceCube** Collaboration, M. Aartsen et al., *JINST* **9** (2014) P03009, [arXiv:1311.4767].

[17] **IceCube** Collaboration, M. Aartsen et al., *Astrophys.J.* **796** (2014), no. 2 109, [arXiv:1406.6757].

[18] **ANTARES** Collaboration, S. Adrian-Martinez et al., *Astrophys.J.* **760** (2012) 53, [arXiv:1207.3105].

[19] J. Braun, J. Dumm, F. De Palma, C. Finley, A. Karle, et al., *Astropart.Phys.* **29** (2008) 299–305, [arXiv:0801.1604].

[20] S. Wakely and D. Horan, *TeVCat: An online catalog for Very High Energy Gamma-Ray Astronomy*, in *Proc. of the International Cosmic Ray Conference*, vol. 3, pp. 1341–1344, 2007.

[21] J. Neyman, *Philosophical Transactions of the Royal Society of London A: Mathematical, Physical and Engineering Sciences* **236** (1937), no. 767 333–380.

[22] **ANTARES** Collaboration, S. Adrian-Martinez et al., *Astrophys.J.* **786** (2014) L5, [arXiv:1402.6182].

[23] K. M. Górski, E. Hivon, A. J. Banday, B. D. Wandelt, F. K. Hansen, M. Reinecke, and M. Bartelmann, *Astrophys.J.* **622** (Apr., 2005) 759–771, [astro-ph/0409513].